Conformation dependent binding of netropsin and distamycin to DNA and DNA model polymers

G. Luck[/], H. Triebel*, M. Waring[≠], and Ch. Zimmer[/]

[/]Akad. Wiss. DDR, Forschungszent. Molekularbiol. und Med., Zentralinst. Mikrobiol. und Exp. Ther., Abt. Biochem., DDR-69 Jena, Beuthenbergstr. 11, GDR

Received 13 February 1974

ABSTRACT

The binding of the antibiotics netropsin and distamycin A to DNA has been studied by thermal melting, CD and sedimentation analysis. Netropsin binds strongly at antibiotic/nucleotide ratios up to at least 0.05. CD spectra obtained using DNA model polymers reveal that netropsin binds tightly to poly (dA) · poly (dT), poly (dA-dT) · poly(dA-dT) and poly (dI-dC) · poly (dI-dC) but poorly, if at all, to poly (dG) · poly (dC). Binding curves obtained with calf thymus DNA reveal one netropsin-binding site per 6.0 nucleotides ($K_a = 2.9 \cdot 10^5\ M^{-1}$); corresponding values for distamycin A are one site per 6.1 nucleotides with $K_a = 11.6 \cdot 10^5\ M^{-1}$. Binding sites apparently involve predominantly A·T-rich sequences whose specific conformation determines their high affinity for the two antibiotics. It is suggested that the binding is stabilized primarily by hydrogen bonding and electrostatic interactions probably in the narrow groove of the DNA helix, but without intercalation. Any local structural deformation of the helix does not involve unwinding greater than approximately 3° per bound antibiotic molecule.

INTRODUCTION

The basic oligopeptide antibiotics netropsin (Nt) and distamycin A (Dst) are known to form extremely stable complexes with double helical DNA (1-7). This is associated with unusually high affinity for dA·T-rich regions (1,4-6). At low ionic strength, the antibiotics interact poorly with RNA (5), polyribonucleotides (1) and more or less strongly with polydeoxyribonucleotides (8,9). However, at moderate to high

ionic strength (> 10^{-1}M Na^+) both oligopeptides show specific binding to DNA with preferential affinity for dA·T-rich regions (5). In view of the findings (10,11) that Dst most probably interferes with specific promotor DNA sequences in the recognition and binding of E.coli RNA-polymerase the competitive binding affinity of these antibiotics to A·T-rich regions is of considerable interest. The principles governing formation of complexes between nucleic acids and the oligopeptides Nt and Dst may thus provide a model relevant to the protein-DNA recognition.

Our present binding data reveal that the antibiotics are tighly bound to dA·T-containing DNA model polymers. The specific conformation of A·T-rich regions appears to determine the complex formation.

MATERIALS AND METHODS

DNA samples are those given by Sarfert and Venner (12). Circular DNA was isolated from bacteriophage PM2 as described earlier (13,14); the preparations contained 80-90% closed circular molecules. Polydeoxyribonucleotides were obtained from P-L. biochemicals, Inc., Milwaukee (Wisc.).

Netropsin and distamycin A were products from cultures of Streptomyces netropsis (5); some of the distamycin A was a preparation from Farmitalia kindly donated by H. Grunicke (Freiburg).

UV absorption and melting measurements were made in a Uvispek spectrophotometer Model H 700; CD spectra were recorded in a Cary 60 spectropolarimeter with the 6001 CD attachment using 1 cm cells. The specific ellipticity [ψ] and molar ellipticity [Θ] are expressed in degrees·ml·g^{-1}·dm^{-1} and degrees·cm^2·$decimoles^{-1}$ as previously calculated (15).

Sedimentation coefficients of antibiotic-DNA complexes were determined at 32000 rev./min at 20° in a Beckman Model E analytical ultracentrifuge with UV optics; complexes with circular PM2 DNA were prepared by method 2 of Waring (14).

Quantitative binding data were determined by the method of "sedimentation dialysis" (16) using the analytical ultracentrifuge equipped with monochromator and photoelectric scanning system. The monochromator was set at a wavelength of

310 nm. Since at this wavelength the absorbancies of free and bound antibiotics differ appreciably, the following procedure was applied: Using the four-hole rotor An-F, two double-sector cells were run simultaneously, one (A) containing the DNA-oligopeptide mixture in the solution sector, the other (B) containing an equally concentrated oligopeptide solution alone. The corresponding solvent sectors were filled with buffer. After the DNA oligopeptide complex had migrated about two-thirds of the distance from the meniscus to the cell bottom, the concentration of free antibiotic was determined from the recorder displacement in the supernatant region centripetal to the boundary in cell (A), whereas the total oligopeptide concentration was determined from the pattern of cell (B).

RESULTS AND DISCUSSION

Optical measurements. Binding of Nt and Dst to DNA is associated with a sharp rise of the melting temperature in the range . to 0.05 moles of oligopeptide/DNA-P as previously shown (1,5,7). A refinement of the melting of the complexes up to a mole ratio of 0.1 is shown in Fig.1 and 2. The absorbance change at 260 nm reflects the helix-coil transition of the DNA complexed with the antibiotics while at 320 nm and 340 nm the release of Nt and Dst, respectively, is indicated (7). Because of some instability of Nt and Dst in aqueous solution possible degradation effects which might occur during heating were followed spectrophotometrically. No changes were observed up to 50°C, while further heating to 98°C caused 2 % loss of the absorbance for Nt and 3 to 4 % absorbance decrease for Dst. The effects are, however, smaller when complexed with DNA. Thus, the measured absorbance changes are not greatly influenced by thermal degradation of the antibiotics. At mole ratios of 0.01 and 0.02 a biphasic melting profile appears at 260 nm. In the first melting step almost no parallel absorbance change can be detected at 320 nm (Fig.1); the decrease at this wavelength coincides with the second melting step at 260 nm. Thus, bound Nt is mainly released when a more strongly stabilized fraction of DNA melts out. At higher ratios than 0.05 the absorbance decrease at 320 nm reveals dissociation of Nt from the complex occurring at temperatures far below the helix-coil transition.

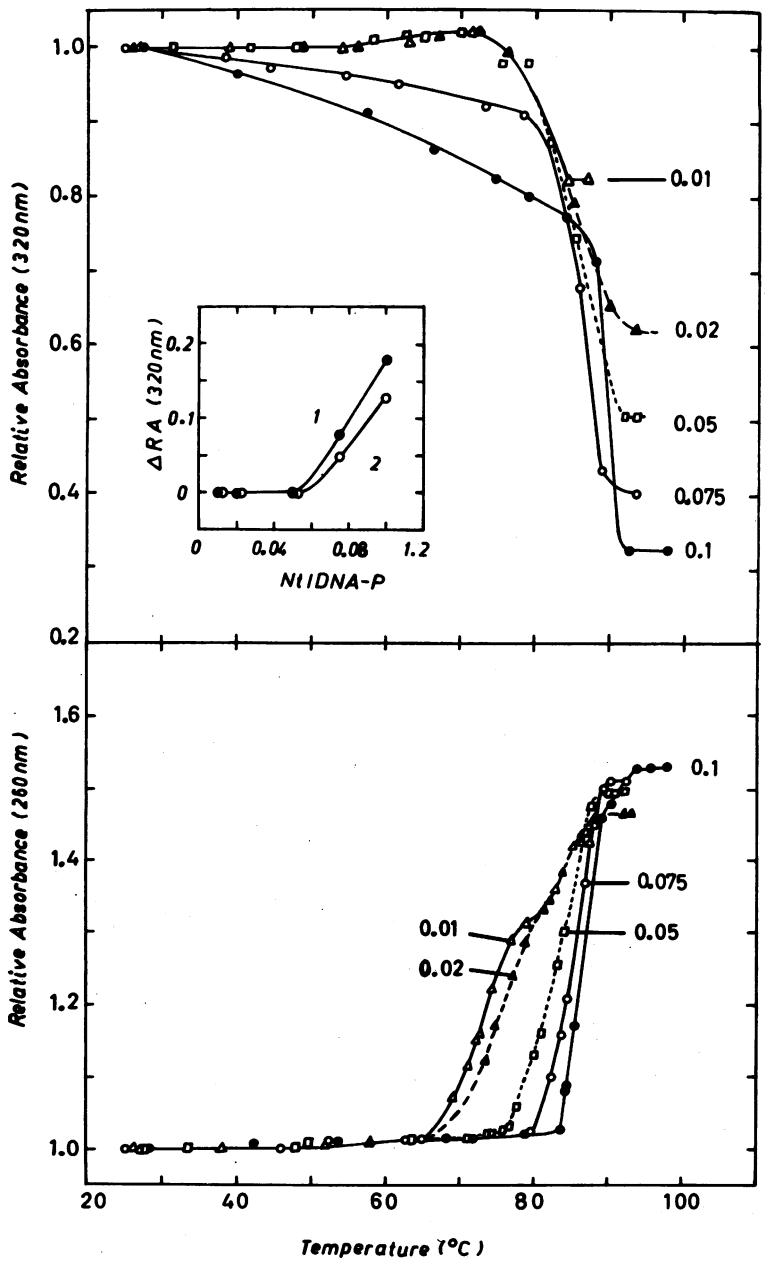

Fig.1 Melting of the calf thymus DNA-Nt complex at 0.02 M Na^+; numbers indicate mole ratio Nt/DNA-P. Insert : Plot of RA (difference in absorbance at 320 nm between 23°C and 75°C) versus Nt/phosphate ratio; 1, calf thymus DNA (58 mole-% A+T); 2, S.maxima (71 mole-% A+T).

This may reflect the existence of different types of binding regions, i.e. thermally unstable complexed sites as well as strong binding sites which dissociate within the helix-coil temperature range. It appears that up to a ratio of 0.05 Nt is associated exclusively with strong binding regions. Similar behaviour with greater resolution of the biphasic melting was observed with the extremely dA·T-rich DNA from Sarcina maxima (71 mole-% A+T). A plot of the absorbance change before the onset of the transition versus mole ratio of Nt/DNA-P is shown in the insert of Fig.1. The released Nt is lower in the case of S.maxima DNA (curve 2) due to the higher AT-content of this DNA. The strongly binding sites for Nt (ratio 0.05) correspond to 1 Nt per 10 base pairs, i.e. 1 Nt per 5.8 AT pairs in calf thymus DNA, a value which is in line with the CD results below.

The melting of the DNA-Dst complex (Fig.2) also shows a biphasic profile at low mole ratios, but the release of Dst molecules below the helix-coil region occurs at 0.1 Dst/DNA-P as indicated by the absorbance decrease at 340 nm. Dst binding to DNA is associated with a different mechanism as indicated by different viscometric behaviour (5).

Since both antibiotics exhibit high affinity for dA·T-rich regions of DNA (4,5,7) we studied the binding to some DNA model polymers. Binding of Dst to some polydeoxyribonucleotides has been reported (9), but the experiments were performed at very low ionic strength, conditions under which one would expect more or less strong interaction of basic oligopeptides with DNA. Thus the specificity of binding could hardly be concluded with certainty. We have tested the binding of Nt to several synthetic DNA polymers at different ionic strengths. At 0.1 M and 0.5 M Na^+ Nt binds tightly to poly (dA)·(dT), poly (dA-dT)·(dA-dT) and poly (dI-dC)·(dI-dC), but weakly or not at all to poly (dG)·(dC). Here we show only the most important melting data for A·T containing polymers with Nt in concentrated salt solution (Fig.3).

Fig.3 demonstrates that even at 4 M NaCl, both poly (dA)·(dT) and poly (dA-dT)·(dA-dT) are stabilized by Nt-binding. Nt is only released from the complex with poly (dA)·(dT) (curve 1 at 325 nm) when melting occurs (curve 1, 260nm). The alternating

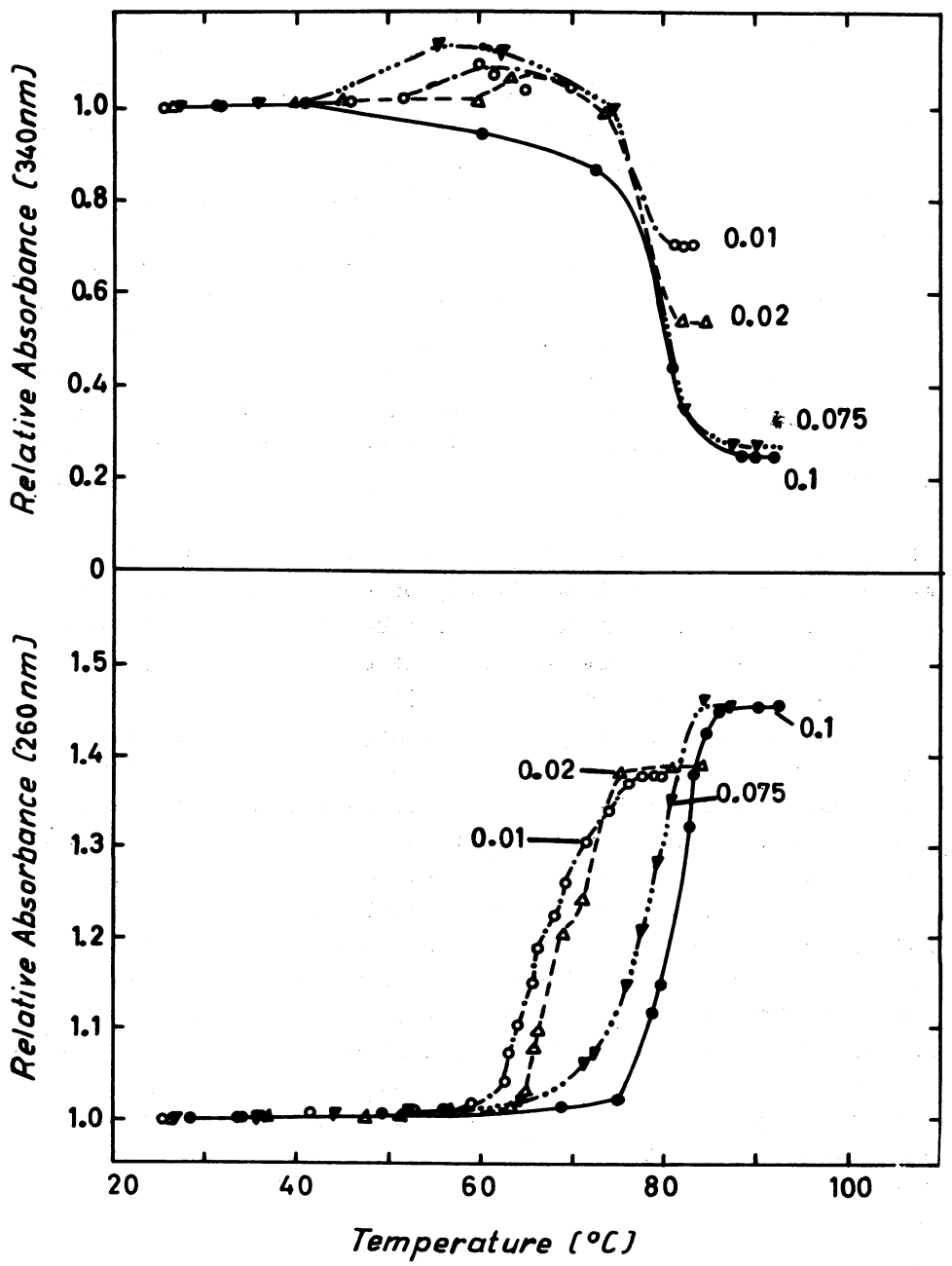

Fig.2 Melting of the Dat-complex of S.maxima DNA (71 mole-% A+T); for conditions see Fig.1.

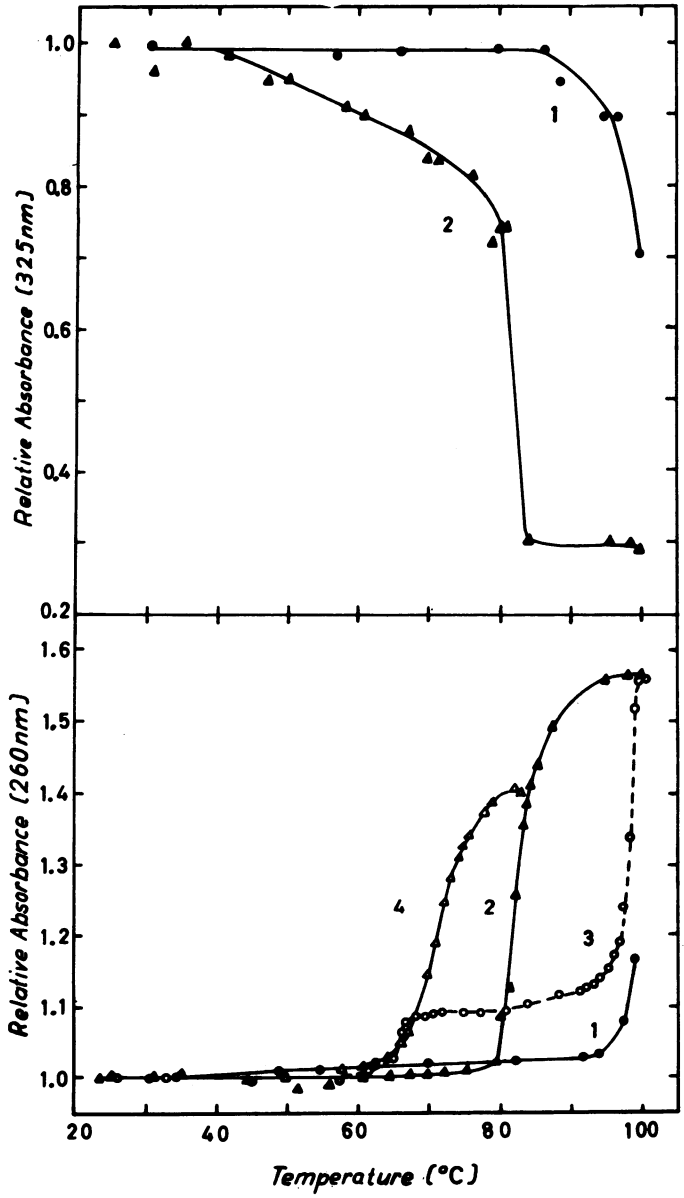

Fig.3 Melting of the Nt-complex of poly(dA)·(dT), 1, and poly (dA-dT)·(dA-dT), 2, in 4 M NaCl at 0.2 Nt/nucleotide; 3 and 4, uncomplexed polymers.

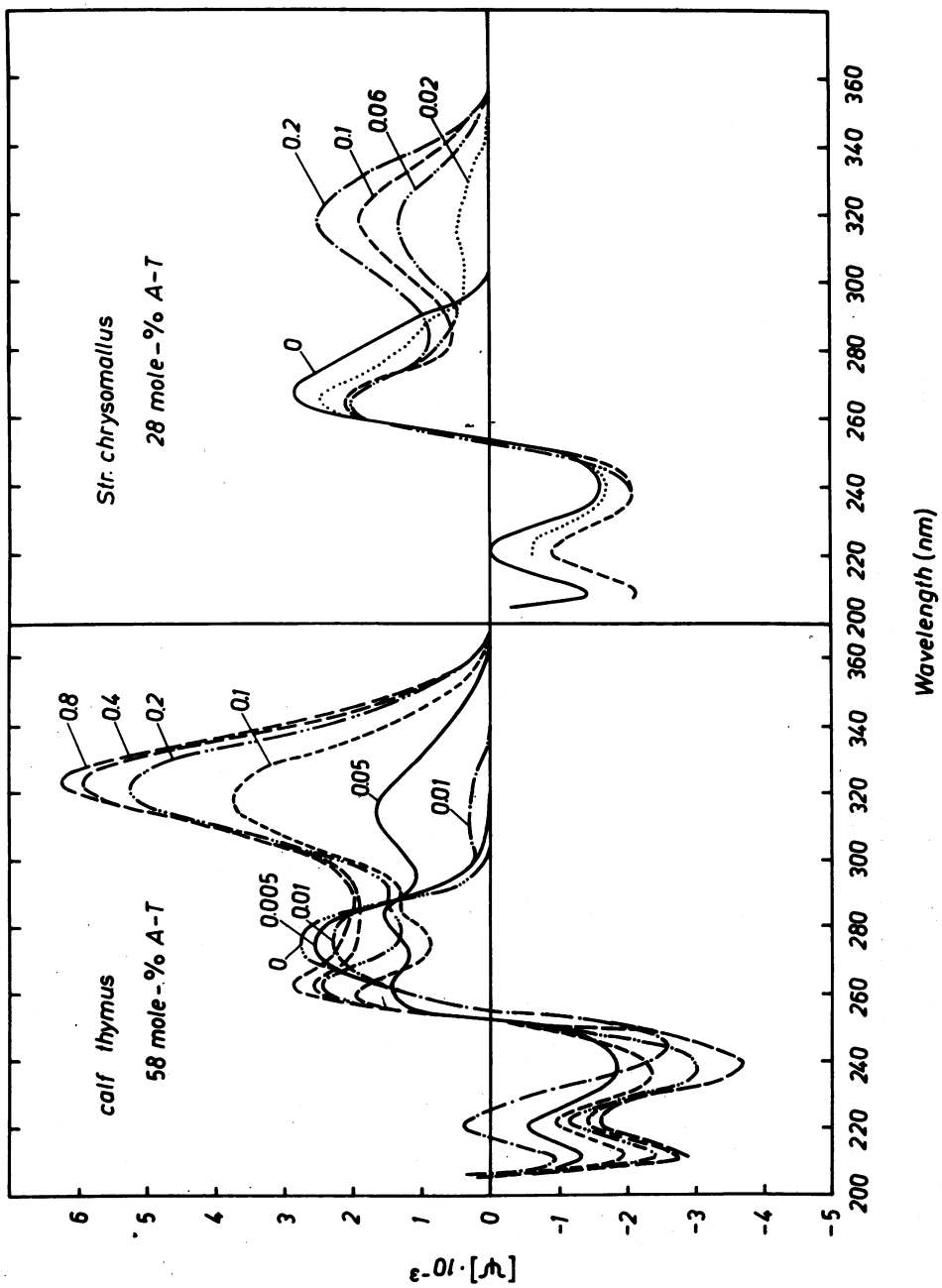

Fig.4 CD of DNA-Nt complexes at 0.02 M NaCl. Numbers indicate the ratio of Nt/DNA-P.

DNA polymer shows a decrease of the absorbance at 325 nm (curve 2) below the melting region indicating the release of bound Nt molecules at 4 M NaCl. At 2 M NaCl (not shown) the release of Nt from the poly (dA-dT)·(dA-dT) complex entirely coincided with the melting region. Since the conformation of the alternating polymer is effectively changed in concentrated salt solutions (17,18) the variation in Nt-binding as reflected in the melting behavior may originate from local variations of the conformation.

The importance of conformation in the binding of Nt and Dst to DNA and model polymers is best demonstrated by CD spectral changes (15). In Fig.4 to 9 we present new Nt binding data. Complex formation between Nt and DNA is accompanied by the appearance of an additional Cotton effect in the long wavelength region reflecting an induced chirality within the structure of bound Nt molecules (15). Fig.4 shows an increasing CD maximum around 320 nm on raising the Nt concentration. This effect is much greater for the A·T-rich DNA than for the G·C-rich one, in agreement with our previous ORD and melting data (1,4,7). There is an isosbestic point at 289 nm valid for the curves up to 0.1 Nt/DNA-P, a mole ratio up to which the binding increases linearly as discussed below (Fig.9). At higher ratios of Nt the CD curves are displaced from this isosbestic point.

The complete lack of any similar induced Cotton effect with double-stranded f2 phage RNA in the presence of 0.1 Nt/RNA-P is demonstrated in Fig.5. A small effect is observable at 0.5 Nt/RNA-P indicating some nonspecific binding. This is, however, achieved only at relatively high local Nt concentration. The picture in Fig.5 reflects effective hindrance of Nt binding to the A conformation, an observation which has been previously made with tRNA and rRNA (4,5). This conclusion is strongly supported by the fact that Nt binding to DNA is effectively diminished when DNA undergoes a transition in ethanolic solution from the B to the A conformation (19).

Comparing the CD results for four DNA model polymers (Figs.6 and 7) at 0.02 M NaCl, strong binding of Nt to poly (dA)·(dT), poly (dA-dT)·(dA-dT) and poly (dI-dC)·(dI-dC) is found while poly (dG)·(dC) shows only weak interaction at

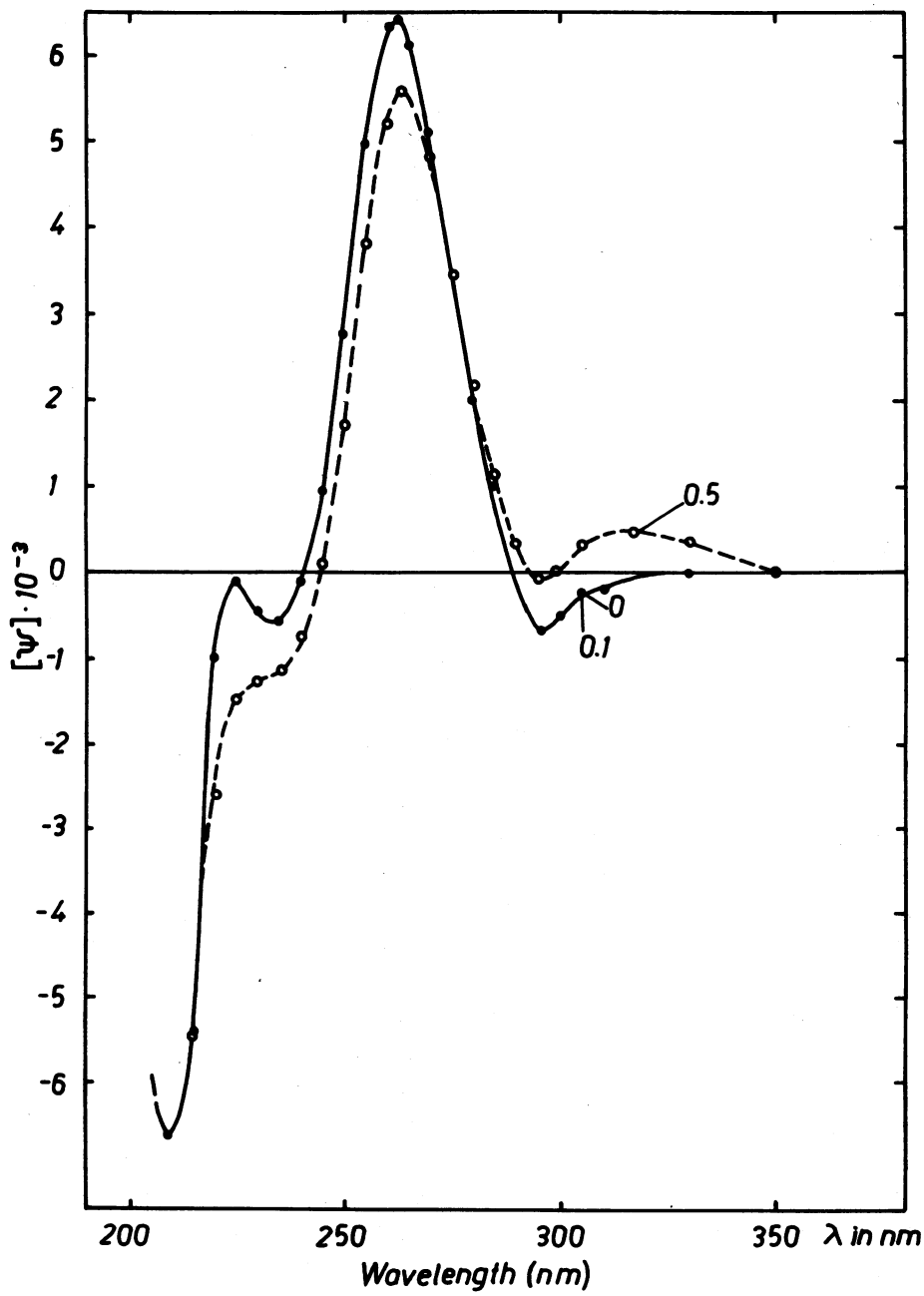

Fig.5 CD of doublestranded RNA from f2 phage in the presence of Nt (mole ratio denoted by numbers) at 0.02 M NaCl.

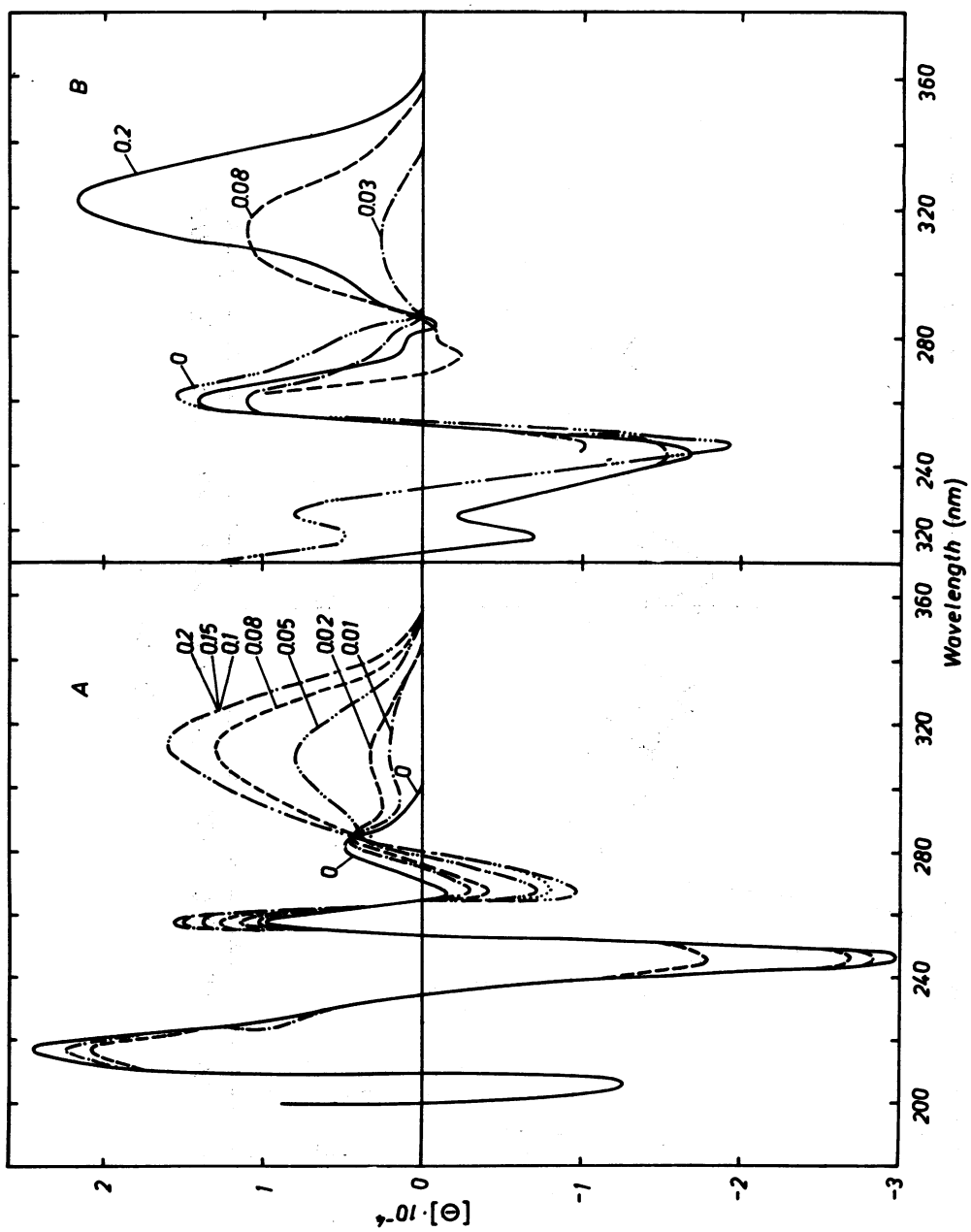

Fig.6 CD of Nt-complexes with A, poly (dA)·(dT) and B, poly (dA-dT)·(dA-dT) at 0.02 M NaCl.

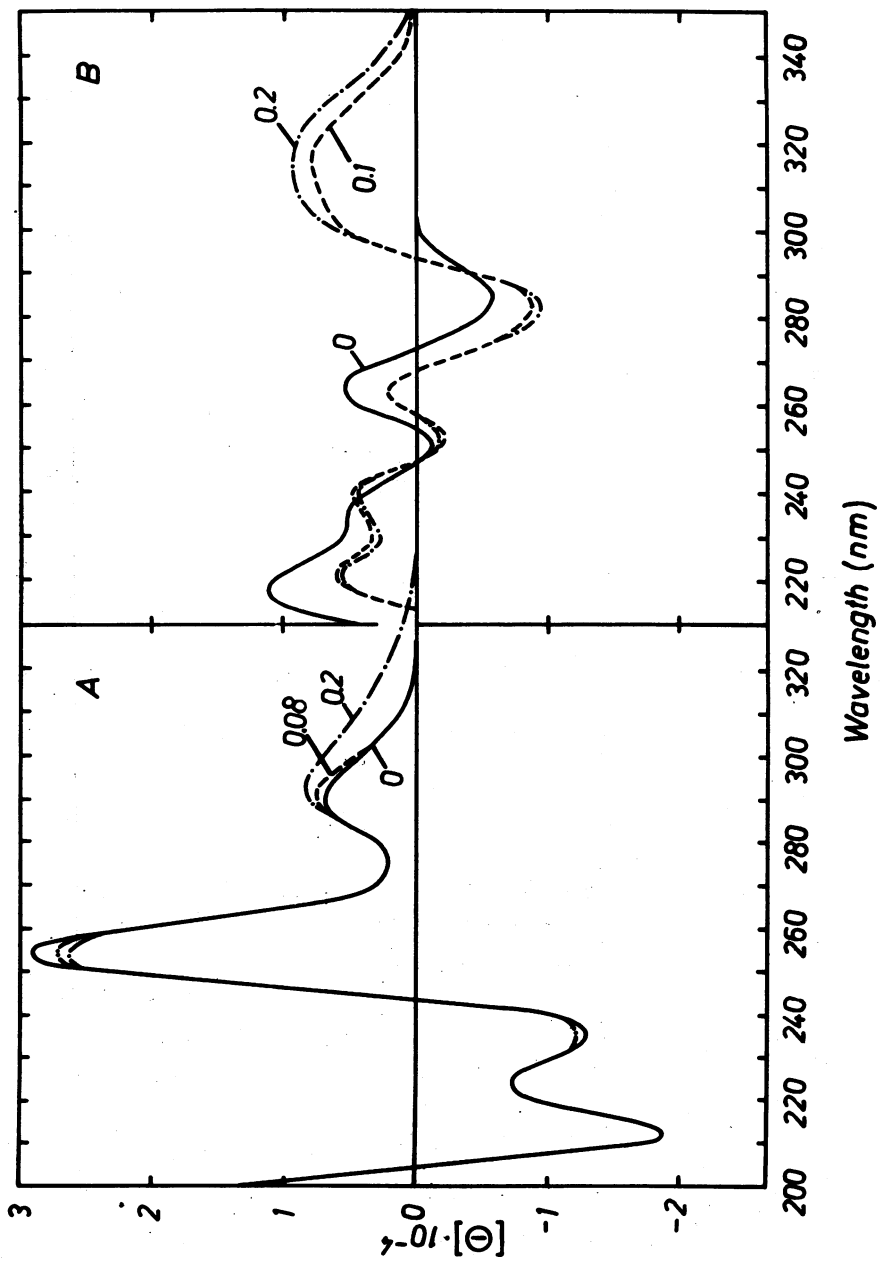

Fig.7 CD of poly (dG)·(dC) at 0.02 M NaCl (A) and of poly (dI-dC)·(dI-dC) at 0.5 M NaCl (B) in the presence of Nt (mole ratio designated by attached numbers).

0.2 Nt/nucleotide (Fig.7); this small effect completely disappeared at 0.1 M NaCl. Poly (dA)·(dT) exhibits a discrete isosbestic point at 285 nm reflecting the formation of a single type of complex. Evidently two distinct conformations exist, that of free $(dA)_n \cdot (dT)_n$ regions and that of complexed sites. For poly (dA-dT)·(dA-dT) the isosbestic point is also present (Fig.6). This strong binding affinity of Nt for dA·T containing model polymers, its lack of interaction with poly (dG)·(dC) and the observed tight binding of Nt to poly (dI-dC)·(dI-dC) (Fig.7) leads to the suggestion that the conformation determines the preferential interaction of Nt at A·T-rich regions of DNA (5,7). Our findings on the lack of a Nt and Dst affinity for the A conformation also imply the importance of geometrical factors (19). Such conformation-dependent effects have already been postulated from recent spectrophotometric results on complexes of Dst with DNA polymers (9).

We have further substantiated the conformation-dependent tight binding of Nt to DNA by CD spectral changes in 5 M LiCl and 4 M NaCl, solvents which are known to cause alterations in the conformation of DNA and model polymers (17,18). Fig.8 clearly indicates a large depression of the binding of Nt to calf thymus DNA in 5 M LiCl while the two A·T-containing polymers are less affected when compared to lower ionic strength (Fig.6). The type of complex formation is not changed as indicated by the presence of isosbestic points in Fig.8. In Fig.9 the observed effects ($[\Theta]_{max}$ and $[\Psi]_{max}$ around 320 nm) are plotted as a function of the mole ratio of Nt added. For poly (dA)·(dT) the binding increases linearly up to a constant value at 0.1 Nt/nucleotide which is consistent with 1 bound Nt per 5 nucleotide-pairs, a value obtained previously in earlier work (20). Poly (dA-dT)·(dA-dT) also exhibits a straight line for Nt binding; however, at higher Nt mole ratios than 0.1 further changes occur which follow a line with smaller slope. The effect of Nt on poly (dI-dC)·(dI-dC) is included for comparison. In the presence of 5 M LiCl the binding of Nt to poly (dA-dT)·(dA-dT) is more affected by the salt than is the case with poly (dA)·(dT). The break in the straight line appears at the same Nt mole ratio of 0.1 as at 0.02 M NaCl. Thus, we believe that

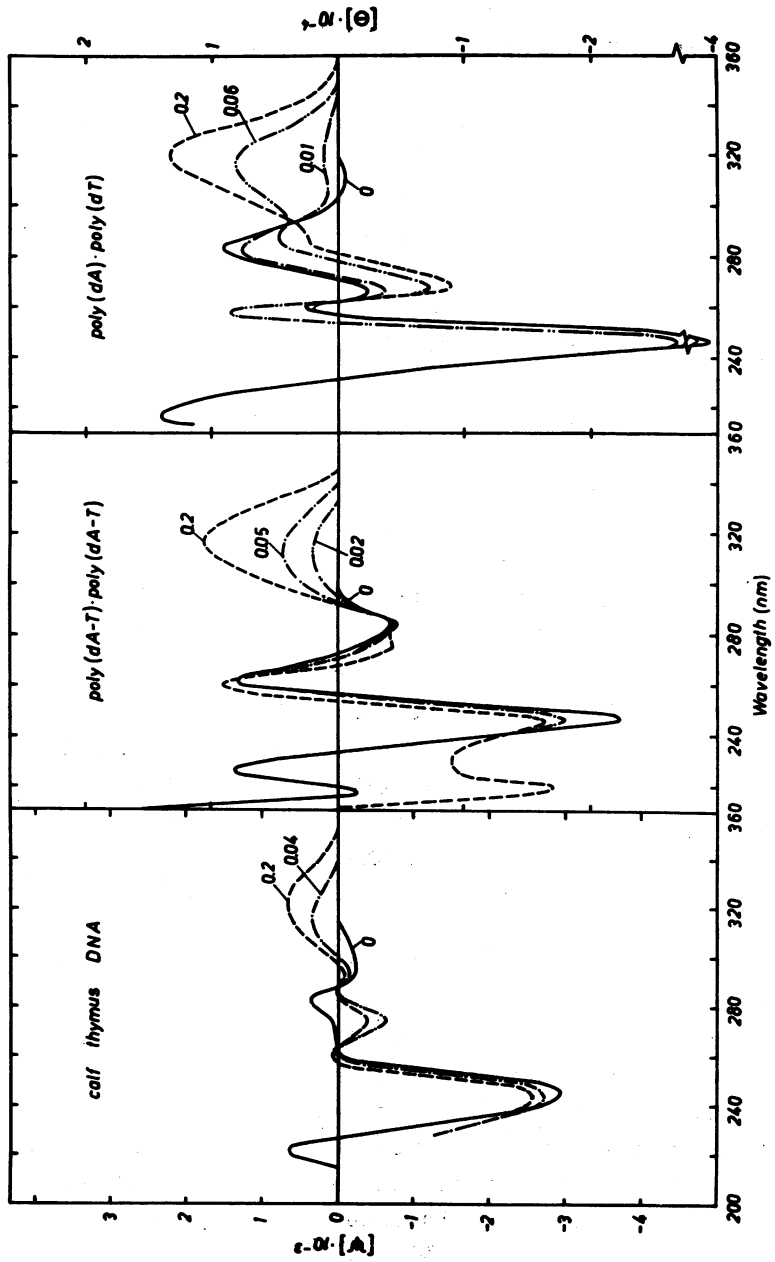

Fig.8 Effect of 5 M LiCl on CD of the Nt-complex with DNA and model polymers. The $[\Theta]\ x10^{-4}$ scale applies to the spectra of the synthetic polynucleotides; the $[\Psi]\ x10^{-3}$ scale applies to that of calf thymus DNA.

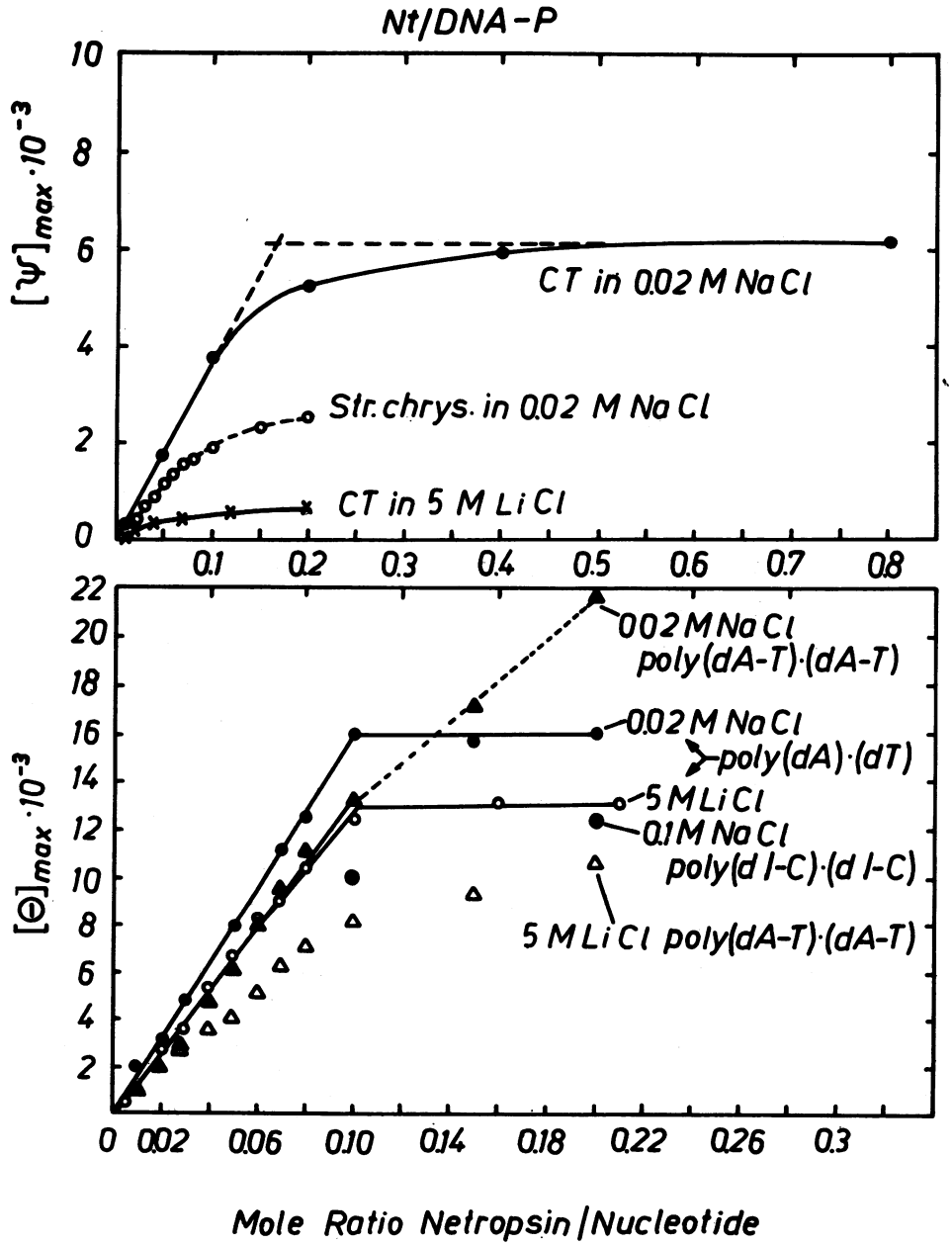

Fig.9 Plots of $[\Psi]_{max}$ and $[\Theta]_{max}$ versus mole ratio Nt/nucleotide; CT-calf thymus, S.chrysom.-Streptomyces chrysomallus.

the type of complex formed is the same under both salt conditions. This similarity very probably reflects a conformational effect which is indicated by our recent observation (17) that the conformation, i.e. the twist angle of the helix is greatly changed for poly (dA-dT)·(dA-dT) in solutions of 5 M LiCl or NaCl but slightly if at all for poly (dA)·(dT). It appears from these considerations and those concerning the inability of Nt to bind to the A conformation that Nt is an indicator for a discrete helical conformation as represented by A·T-rich domains. The recent findings of Bram (21) on X-ray fiber diagrams suggest considerable variations in the geometry of very dA·T-rich helical regions. The thermal melting behaviour of Nt complexes with both A·T containing polymers in 4 M NaCl (Fig.3) is in agreement with the CD results. In the case of calf thymus DNA (Fig.9) the ellipticity increase also follows a straight line up to 0.1 Nt/DNA-P, associated with a characteristic isosbestic point (Fig.4) similar to that observed for the A·T containing polymers (Fig.6). This suggests that a mode of binding similar to that occurring with the polymers is responsible for the induced Cotton effect at 320 nm with DNA (Fig.4), involving an abundance of A·T pairs in those bound DNA sites. The further smooth increase in $[\Psi]$ is indicative of other types of binding regions containing one or two A·T pairs only. In agreement with this suggestion the falloff in the curve for G·C-rich DNA occurs at lower Nt concentration (Fig.9). The point of inflection derived from the two parts of the curve for calf thymus DNA (Fig.9) corresponds to 1 Nt per 3 nucleotide-pairs; if the ellipticity around 320 nm reflects predominantly A·T-rich binding sites involving most of the 58 mole-% A·T pairs we obtain 1 Nt per 5.2 base pairs. This value is close to that estimated for strongly binding sites (5.8 pairs) from melting data in Fig.1. The sharp rise of the melting temperature and the viscosity increase up to 0.05 Nt/DNA-P reported earlier (5,6) as well as the recent findings (22) on the variation of the radius of gyration with Nt concentration, also support our present conclusion. In concentrated LiCl solution, however, binding of Nt to calf thymus DNA is strongly reduced (Figs.8,9) due presumably to salt-induced conformational changes taking place

more effectively for calf thymus DNA than for poly (dA)·(dT) (17). Consequently the small binding curve in 5 M LiCl should represent interaction of Nt with the most tightly-binding dA·T-regions, whose dominating conformation may be determined by $(dA)_n \cdot (dT)_n$ clusters. Recently a high resolution of A·T-rich satellite DNA from Drosophila melanogaster chromosomes has been achieved using a Nt-CsCl gradient (23). Pyrimidine tract analysis suggests that the pentamer $\overset{AATAT}{TTATA}$ is responsible for the Nt binding. These findings accord well with our CD binding data obtained for dA·T containing polymers.

Binding experiments. In the analytical ultracentrifuge a co-sedimentation of Nt and Dst with DNA was observed giving more direct physical evidence for the binding of these antibiotics to DNA. Binding curves evaluated from the sedimentation experiments are shown in Fig.10 where r, the number of moles of antibiotic bound per mole (total) DNA phosphate, is plotted as a function of the concentration of free oligopeptide. At low concentrations of free Nt there is a steep increase of r up to a saturation value. In the region of saturation approximately 0.16–0.17 Nt molecules are bound per nucleotide, i.e. one binding site corresponds to approximately 6 phosphate groups or 3 nucleotide pairs, corresponding to a length of the single phosphate chain of 20 Å. This figure would be compatible with the length of one Nt molecule, neglecting steric factors. Dst shows a similar behaviour to Nt (Fig.10). Again, an approach to a saturation plateau is evident.

In Fig.11 the data of Fig.10 are plotted in the form of [A]/r versus [A] ([A]: molar concentration of nonbound ligand molecules). This special transformation has been chosen because it makes better use of the data obtained at higher concentrations of free ligand than the commonly used Scatchard plot. If the binding process under investigation is based on equivalent and independent binding sites, the ratio [A]/r must be a linear function of [A] (24). Fig.11 shows that, within the limits of experimental error, this requirement seems to be fulfilled by our data. Apparently over the concentration range investigated the binding of Nt (as well as that of Dst) to DNA may be formally described by a single class of binding sites with the same intrinsic binding constant. This result is not necessarily in

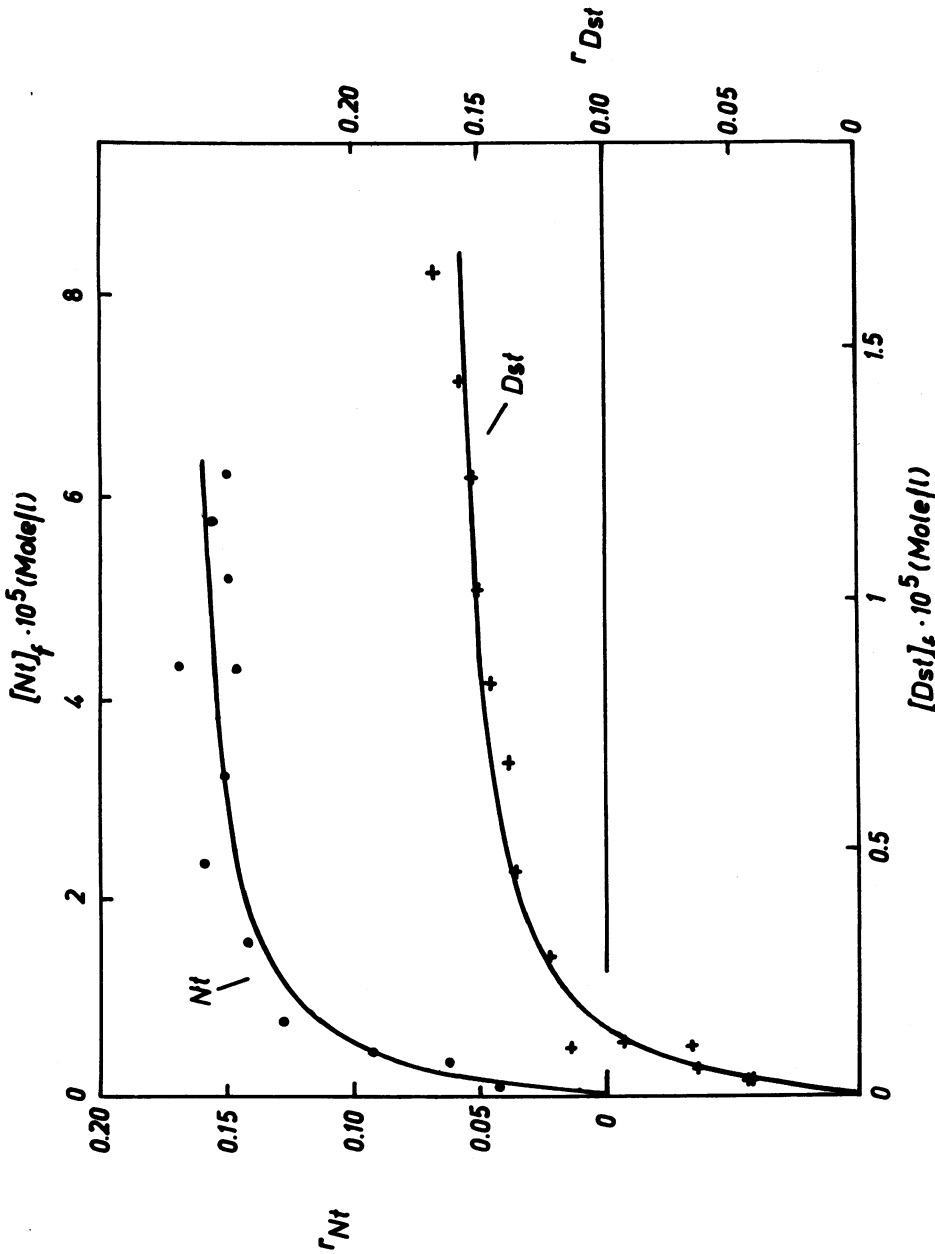

Fig.10 Binding of Nt (o) and Dst (+) to calf thymus DNA in 0.05 M tris-HCl, pH 7.8, as a function of the concentration of free Nt and Dst, respectively.

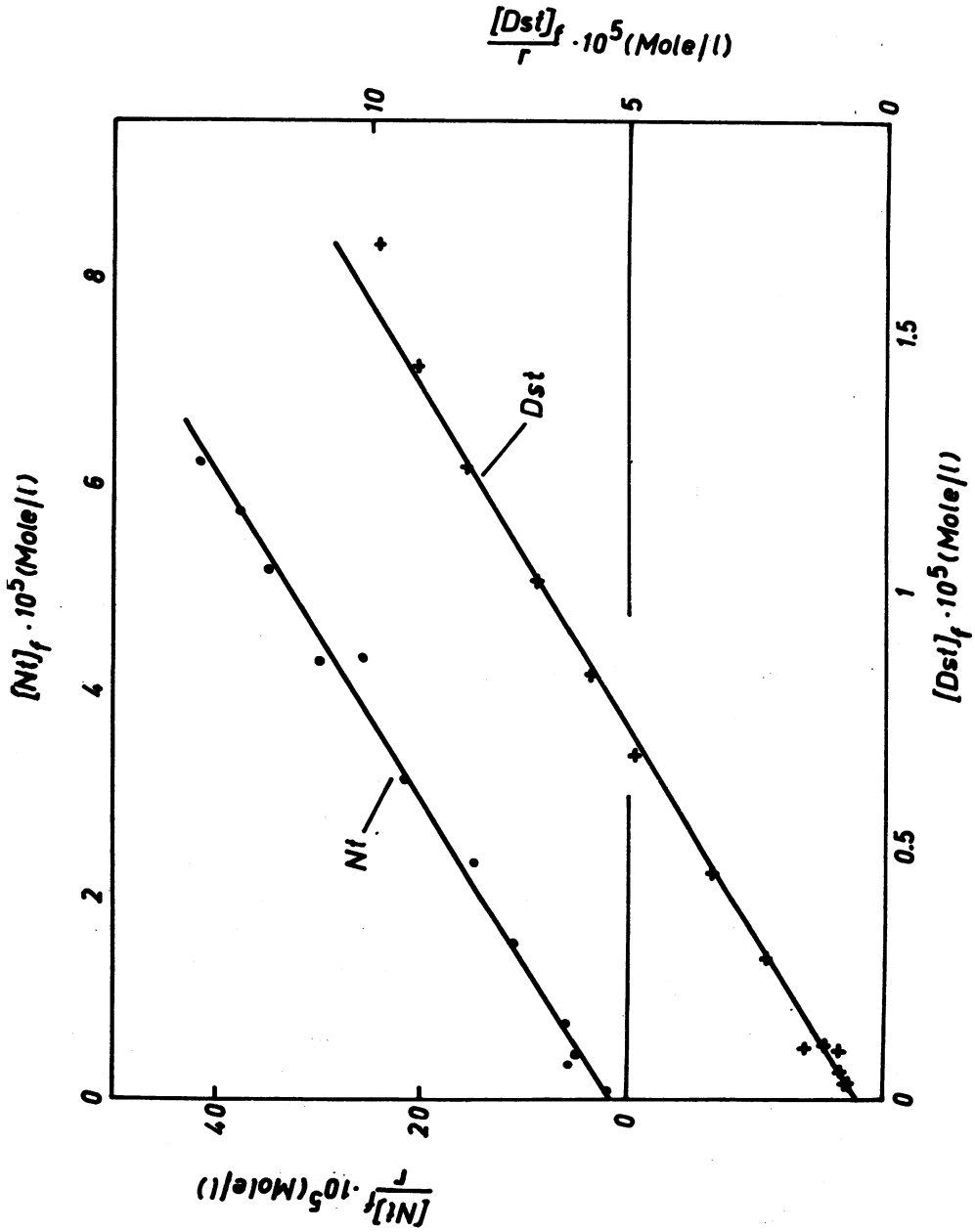

Fig.11 Graphical representation of the binding data of Fig.10 after transformation according to equ. (1).

contradiction with the two main classes of binding sites which were deduced earlier for the DNA-Nt complex (5). It should be noted, however, that the strong A·T-cluster-specific binding of Nt to DNA occurs at very low total Nt/nucleotide ratios and in this respect the data from CD measurements differ from those of the sedimentation analysis. The limited sensitivity of the scanning system of the ultracentrifuge does not permit accurate binding experiments in the range of Nt/DNA-P ratios below 0.05; thus we could not expect to detect the strong A·T specific association process. A similar statement holds for the Dst-DNA complex as will be discussed in more detail below. According to the equation (24)

$$[A]/r = \alpha/K + \alpha\,[A] \qquad (1)$$

the number of phosphate groups per binding site, α, is given by the slope of the straight line in Fig.11, whereas the association constant K (referring to the concentration of binding sites) may be evaluated from the ordinate intercept. A least-squares calculation on the basis of equ. (1) with equal weight given to all points would generally lead to inaccurate binding data, however, because points with relatively high experimental error are disproportionately weighted after the transformation. Therefore best-fitting binding curves for the original data given in Fig.10 were calculated, assuming that the equilibrium is governed by the law of mass action for a single class of independent binding sites. The binding curves drawn in Fig.10 are those calculated with an ICL 1900 computer. In the case of Nt the best fit was obtained with $\alpha = 6.0$ and $K = 2.9 \cdot 10^5\ M^{-1}$, whereas the corresponding values for the DNA-Dst complex are $\alpha = 6.1$ and $K = 11.6 \cdot 10^5\ M^{-1}$. Recently, Mazza et al. (25) have studied complex formation between Dst and SPP1 phage DNA in SSC at extremely low total concentrations of Dst and DNA by using the method of preparative sucrose gradient sedimentation with [^{14}C]-labeled Dst. From the data given in figure 3 of their paper a binding curve r versus $[Dst]_f$ may be constructed which approaches a saturation value of $r_{max} \approx 0.06$ at a concentration of free Dst of some 10^{-8} M. The corresponding linear Scatchard-plot indicates a single class of binding sites. From the best-fitting binding curve we calculated one distamycin-binding site

per 16.1 nucleotides and a very high binding constant of $2.4 \cdot 10^9$ M^{-1}. A combined plot of r versus log $[Dst]_f$ including the measurements of Mazza et al. (25) and our data clearly shows the presence of two independent binding processes with quite different association constants. Unfortunately, both the DNA species and the ionic strength used by Mazza et al. (25) differ from those used by us. Therefore we desisted from treating the combined binding curve on the basis of a model for two classes of sites. Nevertheless, it must be borne in mind that the α value calculated from Fig.10 involves both types of binding sites, while the corresponding K value must be regarded as an apparent association constant deduced from measurements at high ligand concentrations. The real binding constant which describes the second, weaker binding process alone should have a value near $5 \cdot 10^5$ M^{-1}. Similarly the same seems to apply to the α and K values derived from Fig.10 for the Nt-DNA complex since two classes of sites with quite different intrinsic affinity for Nt must likewise be assumed (5). Binding experiments at very low Nt concentrations have not yet been reported.
Since the interaction between Nt and DNA is affected by ionic strength (5), a series of binding measurements was performed in $NaClO_4$ solutions of varying concentration, at a constant Nt (total)/DNA-P ratio of 0.1 and constant DNA concentration. Fig.12 shows that the number of Nt molecules bound per nucleotide clearly decreases with increasing Na^+ concentration, but does not vanish even at a Na^+ concentration of 4 M. From this result it must be concluded that ionic forces actually play an important role in the binding process, but are not solely responsible for the association of Nt with DNA, in line with our CD results discussed above and the ionic strength dependence of T_m (5) and CD of the complexes (20). This conclusion is reinforced by earlier findings (26) that binding of Nt and Dst to DNA is influenced by high salt concentration and urea.

Figs.13 and 14 show the effect of Nt and Dst on circular PM2 DNA. Binding of Nt leads to a small, steady increase in the sedimentation coefficient of both closed and nicked circular molecules. Dst causes a slight increase followed by a gentle decline back almost to the starting values. In neither case does the characteristic, large dip in S_{20} of the closed

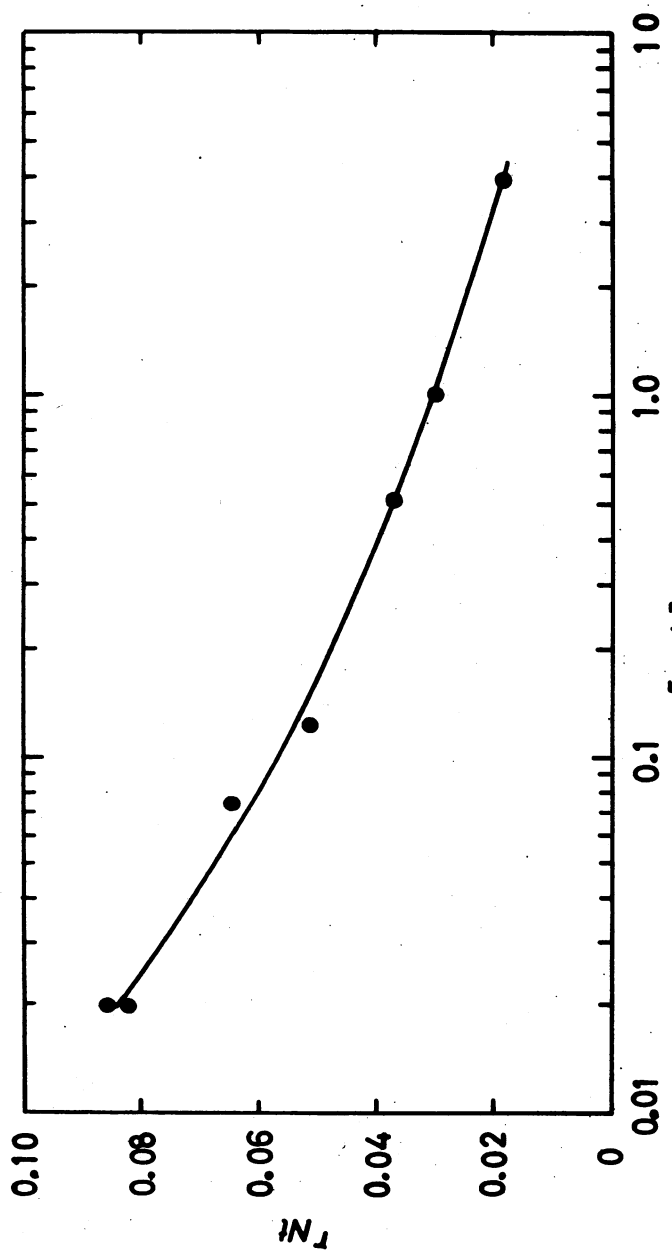

Fig.12 Number of Nt molecules bound per DNA phosphate as a function of Na^+ concentration, at a constant total Nt/DNA-P ratio of 0.1 and constant DNA-P concentration ($9.7 \cdot 10^{-5}$M).

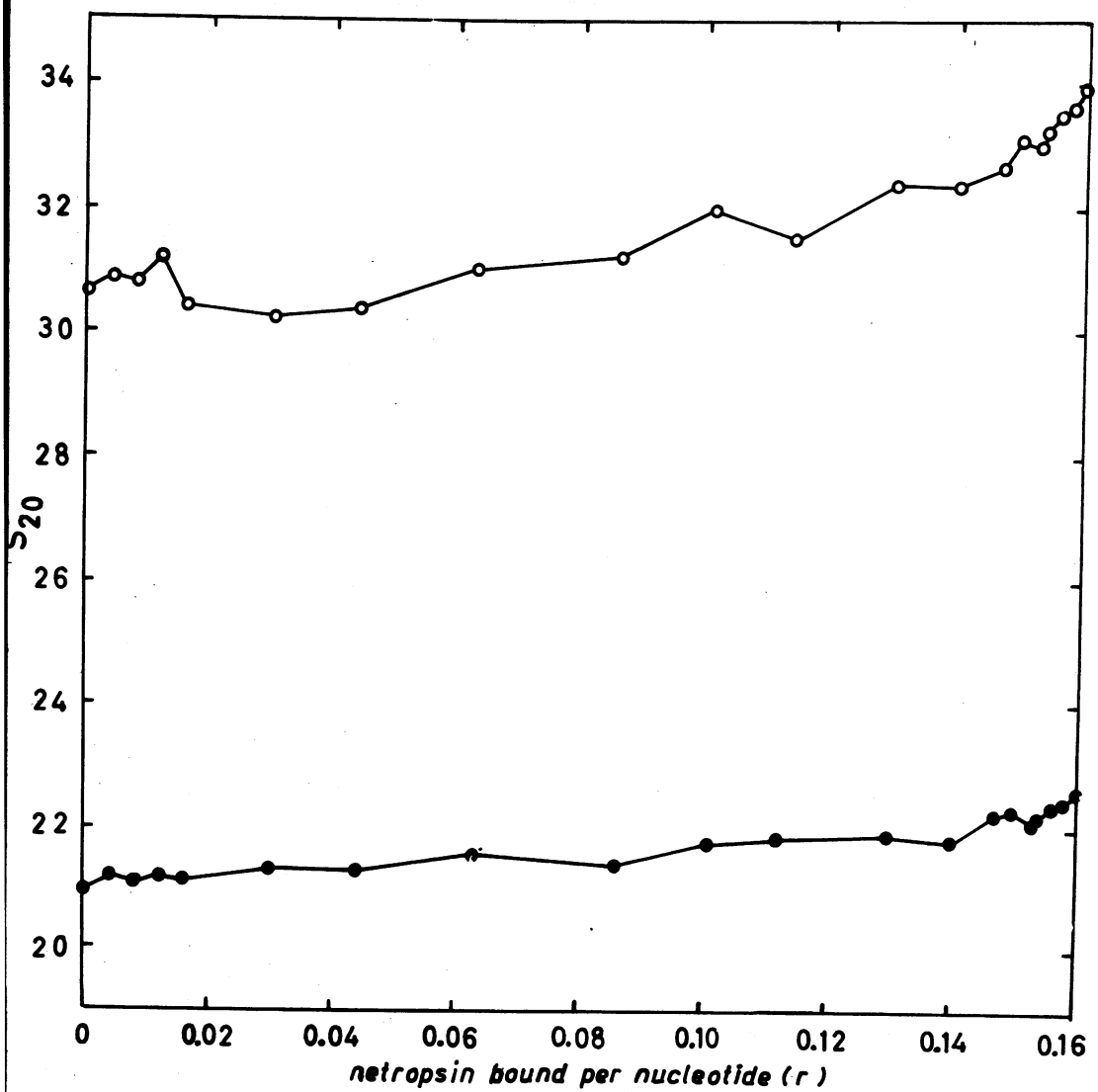

Fig.13 Effect of Nt on the sedimentation coefficient of PM2 DNA in 0.05 M tris HCl buffer pH 7.9. Circles show the S_{20} of closed circular duplex molecules; that of nicked circles is represented by triangles.

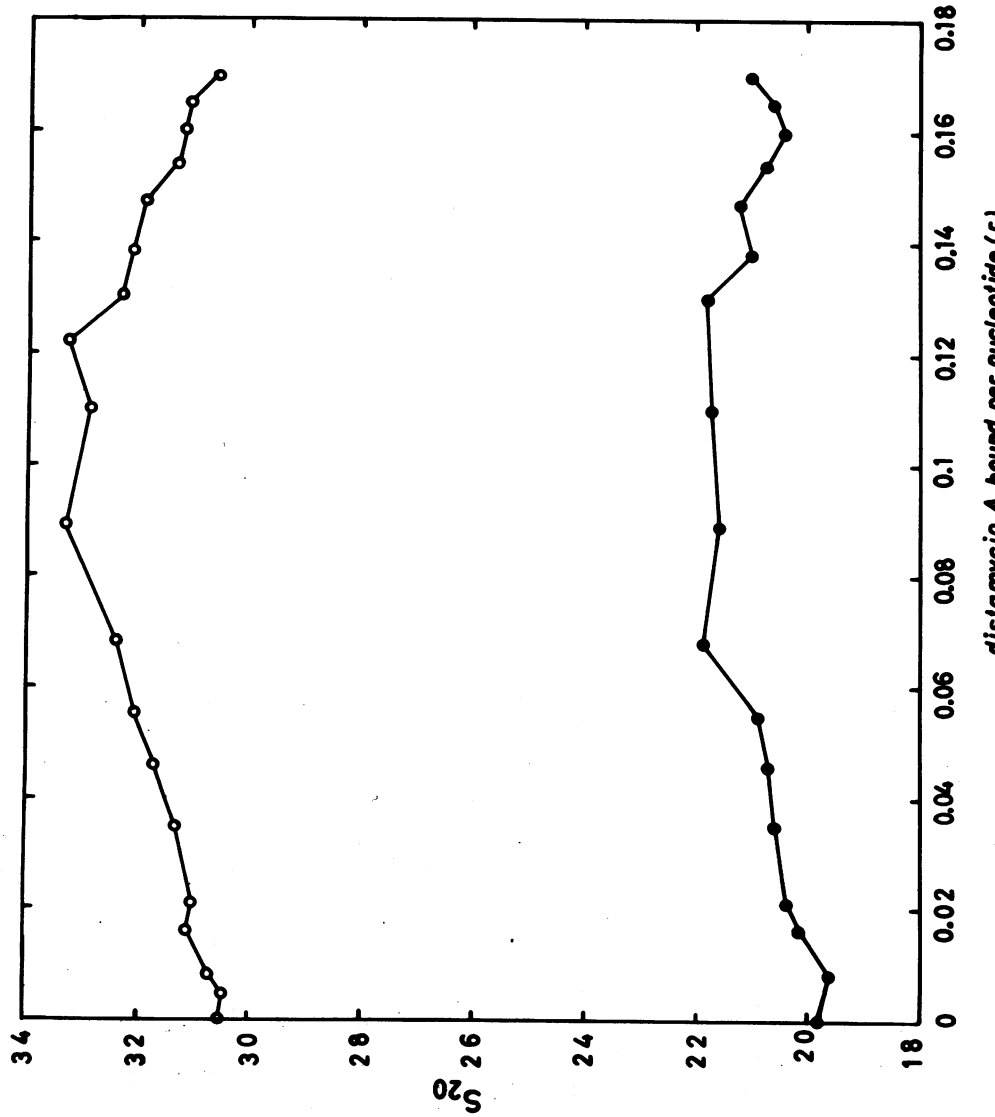

Fig.14 Effect of Dst on the sedimentation coefficient of PM2 DNA. For conditions see Fig.13.

circles caused by intercalating drugs occur, reflecting progressive removal and reversal of the supercoiling (14,27). Evidently therefore the binding of Nt and Dst does not measurably alter the supercoiled state of closed circular DNA and intercalation of the N-methyl pyrrole rings can be ruled out. The highest antibiotic/nucleotide ratios tested were 1:1 in each case, corresponding to virtual saturation of binding sites. In this buffer the dip in S_{20} of the closed circles produced by ethidium bromide centres around a binding ratio of 0.05. Assuming that each ethidium molecule unwinds the DNA helix by 12° (14,27,28) it can be calculated that any unwinding of the DNA helix associated with the binding of one antibiotic molecule cannot exceed 3° for netropsin and 2.8° for distamycin, based on the observation that binding to the levels shown in Figs.13 and 14 produces less effect than the binding of 0.04 molecules of ethidium per nucleotide (29). Recent viscometric measurements on the binding of distamycin to closed circular DNA (9) are in agreement with the conclusion that intercalation does not occur.

Conclusions and binding model: On the basis of the present findings concerning differences in Nt binding to DNA model polymers and its variation in concentrated LiCl solution it is suggested that the conformation of A·T-rich helical segments determines the high binding efficiency. The tightest binding of Nt should occur in a A·T-rich region containing homooligonucleotide clusters of the type $(dA)_n \cdot (dT)_n$. One Nt molecule is bound for every five base pairs, a value which has also been discussed elsewhere (20). Comparing the melting, CD and sedimentation measurements it appears that more than one type of binding may occur for the DNA-Nt complex, i.e. both strong and weak interaction. At least two classes of binding sites were derived from our data and that of Mazza et al. (25) with binding constants of $\approx 5 \cdot 10^5 M^{-1}$ and $2.4 \cdot 10^9 M^{-1}$ for Dst. For Nt binding the corresponding values should be similar. The narrow groove of the helix with an interchain distance of approx. 10 Å, appears more favourable for strong binding of Nt than the wide groove (20). Suggestions concerning groove attachment and a possible binding model have been made previously (20). As evidenced by the results in Figs.13 and 14 attachment of both oli-

gopeptides to the helix takes place without the unwinding required by an intercalation process (26). The results of Reinert (6) on the elongation of Nt-bound A·T-rich DNA from extensive viscosity studies are in close agreement with the present data. His calculated elongation of the DNA contour length by 1.5 Å/Nt implies a profound change in the conformation. The tight binding to predominantly A·T-rich regions in concentrated salt solution can hardly be explained by merely electrostatic attraction as postulated in our previous tentative interpretations (5). We have already surmised (25) that hydrogen bonding as well as other non-ionic forces contribute considerably to the stability of the DNA-complex with Nt as well as with Dst.

Recognition of a A·T-rich helical segment by the oligopeptide molecule most probably occurs through hydrogen bonding besides the long range electrostatic interactions. This is strongly suggested by the effective binding in concentrated salt solution, which is attributed to a specific conformation of A·T-rich sequences. The importance of the guanidino and amidino groups in forming hydrogen bonds is suggested by the following considerations. Elimination of both groups leads to almost complete loss of binding affinity (15), and hydrogen as well as hydrophobic bond-breaking agents cause partial or complete dissociation of the complex (25). As a model for the formation of strong hydrogen bonds by the charged guanidinium ion to phosphate sites and to other hydrogen bond-acceptor sites, the hydrogen-bonded crystal structure of propylguanidinium diethyl phosphate (30) is most informative. According to this model the propylguanidinium ion forms four relatively strong hydrogen bonds (and one weak) directed to three neighbouring phosphate groups in the crystal structure. The charged Nt molecule contains eleven H-donor and three H-acceptor sites which could form an H-bonded complex with a geometrically favourable helical region containing suitably corresponding acceptor-donor sites. Such a situation is present in the narrow groove of the helix (31). There is a great accumulation of oxygens from phosphate and deoxyribose groups facing the narrow groove and all the C(2) = O groups of thymine are free for a contact in this groove. Some van der Waals contacts may also be formed which

would provide further stabilization of the complex and may exclude water from the interaction. A local chirality is induced in the structure of the Nt attached to A·T-rich segments which is accompanied by some perturbation of the B type structure of those regions as discussed previously (15) without, however, any change in the twist angle greater than approximately 3°.

Strong guanidino group-binding to phosphates has been shown to be important in the interaction of arginyl residues of Staphylococcus nuclease with thymidine 3',5'-diphosphate (32) and is probably also involved in the interaction of arginyl side chains in the histone-DNA complex where attachment in the small groove has been suggested (33). With respect to such protein-DNA recognition the dA·T specific binding of Nt to the double helix represents an important model.

ACKNOWLEDGEMENTS

The authors are indebted to Dr.K.E.Reinert for valuable discussions and to DC Ch.Kühne for calculating best-fitting binding curves by means of a general computer program designed by himself. We thank Dr.H.Thrum for providing us with netropsin and Dr.J.Doskocil (Prague) for the generous gift of f2 phage RNA. The excellent technical assistance of Miss Ch.Radtke and Mr.H.Bär and the isolation of DNA by Miss Chem.Ing.E.Sarfert is acknowledged with gratitude.

ADDENDUM

After completion of this paper Dr.R.D.Wells (Madison) kindly provided one of us (M.W.) with his results prior to publication. His data are substantially in agreement with our own.

REFERENCES

1 Zimmer, Ch., Haupt, I. and Thrum, H. (1970) Internationales Symp."Mechanismus of Action of Fungicides, Antibiotics and Cytostatics", held May 1969, Akademie-Verlag, Berlin, pp. 66-69
2 Chandra, P., Zimmer, Ch. and Thrum, H. (1970) FEBS Letters 7, 90
3 Krey, A.K. and Hahn, F.E. (1970) FEBS Letters 10, 175
4 Zimmer, Ch. and Luck, G. (1970) FEBS Letters 10, 339
5 Zimmer, Ch., Reinert, K.E., Luck, G., Wähnert, U., Löber, G. and Thrum, H. (1971) J.Mol.Biol. 58, 329
6 Reinert, K.E. (1972) J.Mol.Biol. 72, 593
7 Zimmer, Ch., Puschendorf, B., Grunicke, H., Chandra, P. and

Venner, H. (1971) Eur. J. Biochem. 21, 269
8 Zimmer, Ch. (1972) studia biophysica 31/32, 447
9 Krey, A.K., Allison, G. and Hahn, F.E. (1973) FEBS Letters 29, 58
10 Puschendorf, B., Petersen, E., Wolf, H., Werchau, H. and Grunicke, H. (1971) Biochem. Biophys. Res. Communic. 43,617
11 Böhlandt, D., Puschendorf, B. and Grunicke, H. (1973) Abstract, Meeting of the Biochem. Gesellschaften der BRD, Schweiz u. Österreich, Innsbruck
12 Sarfert, E. and Venner, H. (1969) Z.Allg.Mikrobiol. 9, 753
13 Espejo, R.T., Canelo, E.S. and Sinsheimer, R.L. (1969) Proc. Natl. Acad.Sci. U.S. 63, 1164
14 Waring, M. (1970) J.Mol.Biol. 54, 247
15 Zimmer, Ch., Luck, G., Thrum, H. and Pitra, Ch. (1972) Eur. J.Biochem. 26, 81
16 Steinberg, I.Z. and Schachman, H.K. (1966) Biochemistry 5, 3728
17 Zimmer, Ch., and Luck, G., submitted
18 Studdert, D.S., Patroni, M. and Davis, R.C. (1972) Biopolymers 11, 761
19 Luck, G. and Zimmer, Ch., (1973) studia biophysica 40, 9
20 Zassedatelev, A.S., Gursky, G.V., Zimmer, Ch. and Thrum, H. (1972) Abstracts Internat. Biophys. Congr., Moscow, vol.2, 253
21 Bram, S. (1973) Proc. Nat. Acad. Sci. USA 70, 2167
22 Strassburger, J. (1974) studia biophysica, in press
23 Peacocke, W.J., Brutlag, D., Goldring, E., Appels, R., Hinton, C.W. and Lindsley, D.L. (1973) Cold Spring Harbor Symp. Quant.Biol.
24 Klotz, I.M. and Hunsten, D.L. (1972) Biochemistry 10, 3065
25 Mazza, G., Galizzi, A., Minghetti, A. and Siccardi, A. (1973) Antimicrob. Ag. Chemother. 3 384-391
26 Zimmer, Ch. and Luck, G. (1973) Biochem. Biophys. Acta 312, 215
27 Waring, M.J. (1972) The Molecular Basis of Antibiotic Action by E.F.Gale, E. Cundliffe, P.E. Reynolds, M.H.Richmond and M.J. Waring, Wiley, London, pp 173-277.
28 Fuller, W. and Waring, M.J. (1964) Ber.Bunsenges. Physik. Chem. 68, 805-808
29 Müller, W., Crothers, D.M. and Waring, M.J. (1973) Eur. J. Biochem. 39, 223-234
30 Furberg, S. and Solbank, J. (1972) Acta Chem. Scand. 26, 3699
31 Lewin, S. (1967) J. Theoret. Biol. 17, 181
32 Cotton, F.A., Huzen, E.E., Day, V.W., Larsen, S., Norman, J.G., Wong, S.T.K. and Johnson, K.H. (1973) J.Amer.Chem. Soc. 95, 2367
33 Feughelman, M., Langridge, R., Seeds, W.E., Wilkins, M.H.F., Barclay, R.K. and Hamilton, L.D. (1955) Nature 175, 834

* Akademie der Wissenschaften der DDR, Forschungszentrum fur Molekularbiologie und Medizin, Zentralinstitut fur Mikrobiologie und Experimentelle Therapie, Abteilung Biophysikochemie, DDR-69 Jena, Beuthenbergstr.11, GDR

Department of Pharmacology, University of Cambridge Medical School, Cambridge CB2 2QD, England